NASA-CR-201110

Revised Oct '95

Non-Parabolic Hydrodynamic Formulations for the Simulation of Inhomogeneous Semiconductor Devices

Arlynn W. Smith and Kevin F. Brennan
School of Electrical and Computer Engineering
and
Microelectronics Research Center
Georgia Institute of Technology
Atlanta, GA 30332-0250

ABSTRACT

Hydrodynamic models are becoming prevalent design tools for small scale devices and other devices in which high energy effects can dominate transport. Most current hydrodynamic models use a parabolic band approximation to obtain fairly simple conservation equations. Interest in accounting for band structure effects in hydrodynamic device simulation has begun to grow since parabolic models can not fully describe the transport in state of the art devices due to the distribution populating non-parabolic states within the band. This paper presents two different non-parabolic formulations of the hydrodynamic model suitable for the simulation of inhomogeneous semiconductor devices. The first formulation uses the Kane dispersion relationship $(\hbar k)^2/2m = W(1 + \alpha W)$. The second formulation makes use of a power law $\{(\hbar k)^2/2m = xW^y\}$ for the dispersion relation. Hydrodynamic models which use the first formulation rely on the binomial expansion to obtain moment equations with closed form coefficients. This limits the energy range over which the model is valid. The power law formulation readily produces closed form coefficients similar to those obtained using the parabolic band approximation. However, the fitting parameters (x,y) are only valid over a limited energy range. The physical significance of the band non-parabolicity is discussed as well as the advantages\disadvantages and approximations of the two non-parabolic models. A companion paper describes device simulations based on the three dispersion relationships; parabolic, Kane dispersion, and power law dispersion.

NOMENCLATURE

W	Carrier Energy
$\hbar$	Planck's constant divided by 2π
k	Reciprocal lattice vector
α	Non-parabolicity factor under the Kane dispersion relation, positional dependent
m	Carrier mass at the band edge, a constant but positional dependent
x, y	Adjustable parameters for the power law dispersion relation, both positional dependent
$g(k)$	Density of states in momentum space
W_e	Conduction band edge
E_f	Electron quasi-fermi level
K_b	Boltzmann's constant
T_e	Electron temperature
F_γ	Fermi integral of various order
$\mathcal{F}_\gamma$	Fermi integral divided by Gamma function
Γ	Gamma function
N_c	Effective density of states
η	Reduced energy $\{(E_{fn}-E_c)/(KT_e)\}$
E_g	Semiconductor band gap
∇, ∇_r	Gradient operator in physical space
∇_k	Gradient operator in k space
v_g	Group velocity
f	Distribution function
f_o	Equilibrium distribution function
τ	Relaxation time
ε_c	Conduction band potentials (electrostatic, affinity, and band gap narrowing)
n	Electron concentration
I	Identity matrix

$$g = \frac{1}{2\pi^2}\left(\frac{2m_e}{\hbar^2}\right)^{\frac{3}{2}} \qquad \Psi = 1+2\alpha W \qquad \Upsilon = 1+\alpha W$$

$$\Omega = \left(\mathcal{F}_{\frac{1}{2}} + \frac{15}{4}\alpha KT_e \mathcal{F}_{\frac{3}{2}}\right) \qquad \Lambda = \left(\mathcal{F}_{-\frac{1}{2}} + \frac{15}{4}\alpha KT_e \mathcal{F}_{\frac{1}{2}}\right)$$

INTRODUCTION

The use of hydrodynamic models for device simulation are becoming common as characteristic device dimensions continue to decrease. Hot electron effects can play a dominant role in carrier transport for high mobility semiconductors. Current hydrodynamic models consist of a set of conservation equations derived by taking moments of the Boltzmann transport equation (BTE). During the derivation of the conservation equations the parabolic band approximation is used to obtain rather simple coefficients on the forcing terms in the flux equations. By relying on the parabolic band approximation higher order energy transport effects due to variation in the band structure are neglected. Interest in accounting for band structure effects in hydrodynamic device simulation has begun to grow because parabolic models can not adequately account for high energy effects in semiconductors with non-parabolic band structures. Non-parabolic band formulations have a history dating back to the 1950's [1-3]. However drift-diffusion models and more specifically hydrodynamic simulators with non-parabolic band formulations are a very recent topic of research.

Several non-parabolic hydrodynamic models have been reported for homogeneous material systems [4-7] using the Kane dispersion relationship [3]. The general functional form obtained is similar to parabolic hydrodynamic models with first order corrections on the diffusion term. Azoff [8] derived a hydrodynamic model suitable for degenerate heterostructure semiconductors though the final form of the equations was not directly amenable to current device simulation codes. However, Azoff clearly showed that a forcing term due to a gradient in the non-parabolicity factor exists. Woolard et. al. [9] presented a non-parabolic hydrodynamic model based on moments of the velocity and energy (u, W(k)) instead of the momentum and momentum squared ($\hbar k$, $\hbar^2 k^2$). This leads to a simpler energy conservation equation. However, the non-parabolic coefficient in the field term and the forcing terms due to non-uniform band structure were neglected in the other moment equations. Cassi and Riccò [10] introduced an alternative to the Kane relation in the form of a power law for the dispersion relationship. Instead of using the classical Kane dispersion law relating the energy and momentum, the band was fit over a specified energy range using two adjustable parameters. The approximations and assumptions implied by assuming the power law formulation were absent. It will be shown below that the power law formulation of the dispersion relation leads to a more simplistic and compact formulation than the classical Kane expression.

The purpose of this paper is to introduce two non-parabolic hydrodynamic formulations suitable for the simulation of devices with inhomogeneous material layers. The final form of the conservation equations will be in a form which will allow incorporation into existing device simulation codes, similar to the parabolic formulation. These different formulations are based on different choices for the dispersion relationship, one uses the standard Kane dispersion for non-parabolic bands and the second uses a power law relationship [10]. For comparison the parabolic hydrodynamic formulation will also be presented. The form of the conservation equations are strongly affected by the non-parabolicity factor of the bands, the choice of the dispersion relationship, and the assumptions made to simplify the coefficients. As in the case of the parabolic formulation, both non-parabolic formulations require estimates of higher order moments to provide mathematical closure of the relationships. It will be shown that more physical insight can be obtained by examining the terms from the power law formulation due to their similarity to the parabolic formulation. The power law is advantageous in that the terms of the conservation equations are the same as in the parabolic formulation, except for a simple multiplicative constant when Boltzmann statistics are employed.

Dispersion Relations and Carrier Concentration

The two non-parabolic dispersion relations relating the energy to the momentum are

$$W(1+\alpha W)=\frac{(\hbar k)^2}{2m} \qquad\qquad xW^{y}=\frac{(\hbar k)^2}{2m} \tag{1}$$

Where α is the non-parabolicity factor in the Kane dispersion relation. This parameter is usually calculated from a k•P perturbation approach to the band structure. The α factor can also be estimated in terms of known parameters of the semiconductor [10]. The second non-parabolic dispersion relation is the power law formulation of Cassi and Riccò [10] which is not a first order approach to the band structure as compared to the Kane dispersion relation. Instead, the parameters x and y are obtained by a best fit to equation (1a) over a specified energy range. In reference [10] this energy range was (1.5 eV, 3.0 eV) and the authors produced a very good fit for $\alpha = 0.4789$, determined by inference from x and y and is reproduced in Figure 1. The formulae for the carrier concentration using these two dispersion relations and assuming Fermi-Dirac statistics are (the binomial expansion has been employed for equation (2a))

$$n = N_c(T_e)\left[\mathfrak{F}_{\frac{1}{2}}(\eta) + \frac{15}{4}\alpha K_B T_e \mathfrak{F}_{\frac{3}{2}}(\eta)\right] \qquad n = N_c(T_e) x^{\frac{3}{2}} y (K_B T_e)^{\frac{3}{2}(y-1)} \left[\frac{\Gamma(\frac{3}{2}y)}{\Gamma(\frac{3}{2})} \mathfrak{F}_{\frac{3}{2}y-1}(\eta)\right] \quad (2)$$

In the case of the Kane dispersion the non-parabolicity is a perturbation to the parabolic model regardless of the fact that Fermi-Dirac statistics were used in the derivation instead of Boltzmann statistics. In the power law case, unlike the α formulation, the carrier concentration will only differ from the parabolic by a multiplicative constant if Boltzmann statistics are assumed.

Within the hydrodynamic simulation of a device the carrier concentration is calculated by directly solving the continuity equations. Inspection of equations (2a) and (2b) shows that the concentration in both cases is a function of the reduced energy, η. The determination of η at each position is crucial to the successful simulation of a device since most of the factors within the transport equations i.e. number of ionized dopants, Shockley-Read-Hall recombination etc., are functions of η as well. Therefore, from the knowledge of the carrier concentration at any specific position the reduced energy, η, is calculated by suitably inverting equations (2a) and (2b). With these facts in mind it is illustrative to compare the non-parabolic formulations for the carrier concentration to the parabolic formulation at various reduced energy values. Figure 2 displays the deviation from the parabolic formulation for $\alpha = 0.4789$, $x = 1.365$, and $y = 1.52$ [10]. The case of the full Kane dispersion relation before binomial expansion is also given in Figure 2 and shows that the binomial expansion is justified for this case of the non-parabolicity parameter; the two curves are almost identical throughout the entire reduced energy range. Notice also that the deviation of the alpha nonparabolicity formulations is at most 5% from the parabolic case until the reduced energy exceeds zero, when the difference in the orders of the Fermi integral is larger. However, in the case of the power law fit at high energy, the deviation from the parabolic case is more than 82% and more than 87% from the α formulation. To explain this large difference the plots of the dispersion relations must be re-examined, Figure 1. At the high energy part of the curve the power law and α formulations have nearly identical dispersion relations. The insert in Figure 1 shows the low energy range and shows the maximum deviation of the two curves. Though there is a greater deviation between the two curves at lower energy than at high energy, the maximum difference between the two curves is insufficient by itself to fully account for the large difference in the carrier concentrations. However, carrier concentration depends upon both the density of states and the distribution function. Since the distribution function weights more heavily to lower energy states, a mismatch at low energy is strongly reflected in the product of the distribution function times the density of states and subsequently the carrier concentration. Therefore, in order to obtain a matched value of the carrier concentration, it is critical to have a closer fit to the low energy range of the band. For comparison, a low energy fit was made using a different set of for x and y, $x = 1.185$ and $y = 1.052$. These values of x and y were determined by fitting the power law dispersion relation over the low energy range ($0.0 \text{ eV} \leq W \leq 0.2 \text{ eV}$). As can be seen from the inset of Figure 1, the dispersion relations match very closely at low energy but deviate significantly at higher energy. Figure 2 also shows the calculated carrier concentrations for various reduced energy values using the low energy power law fit factors. Compared to the power law fit to the high energy range, using the power law fit to the low energy range of the band produces concentration values which closely match those obtained using the α formulation.

Particle Flux Equations

The general flux ($\Theta = v_g$) conservation equation is determined by taking moments of the BTE as

$$\begin{aligned} &\frac{\partial}{\partial t}\left(\overline{v_g f}\right) + \nabla_r \cdot \left(\overline{f v_g v_g}\right) - f\frac{\hbar^2 (kk)}{m(k)} \cdot \nabla_r\left(\frac{1}{m(W)}\right) \\ &- f\overline{F} \cdot \frac{1}{m(k)}\mathrm{I} + f\overline{F} \cdot \frac{3(k\nabla_k m(k))}{m(k)^2} = \overline{v_g}\frac{-(f-f_0)}{\tau} \end{aligned} \tag{3}$$

Notice that the third, fourth and fifth terms on the left hand side are tensor products. The factor of 3 in the fifth term is due to the order of parenthesis in the original moment equation. This moment equation can not be processed further until some functional form of the effective mass is assumed, which depends on the choice of the dispersion relation. Using the parabolic dispersion and the two dispersion relations in equation (1), the resulting flux equations are (positional subscript on the gradient operators has been removed)

$$\frac{\partial}{\partial t}\left(\overline{v_g f}\right) + \frac{2}{3m_e}\nabla(fW) + \nabla\epsilon_c\frac{f}{m_e} - \frac{\nabla m_e}{m_e^2}fW = \overline{v_g}\frac{-(f-f_0)}{\tau} \tag{4}$$

$$\frac{\partial}{\partial t}\left(\overline{v_g f}\right) + \frac{2}{3m_e}\nabla\left(f\frac{W\Upsilon}{\Psi^2}\right) - \left(f\left[1+\frac{4}{3}\alpha W\Upsilon\right]\frac{W\Upsilon}{\Psi^4}\right)\frac{\nabla m_e}{m_e^2} + \left(f\frac{W^2\left(-1+\frac{4}{3}\Upsilon^2\right)}{m_e\Psi^4}\right)\nabla\alpha + \left(\frac{f}{m_e\Psi^3}\right)\nabla\epsilon_e = \overline{v_g}\frac{-(f-f_0)}{\tau} \tag{5}$$

$$\frac{\partial}{\partial t}(\overline{\upsilon_g f}) + \frac{2}{3m_e x y^2}\nabla(fW^{2-y}) + \left[\frac{\nabla m_e}{m_e} + \frac{\nabla x}{x}\right]\frac{fW^{2-y}(y-4)}{3m_e x y^3} + \left(\frac{fW^{1-y}}{m_e x y}\right)\left(\frac{2}{y}-1\right)\nabla\epsilon_c$$
$$+ \left(\frac{fW^{2-y}}{m_e x y^3}\right)\left(-\frac{2}{3}(1+2\ln(W)) + y\ln(W)\right)\nabla y = \overline{\upsilon_g}\frac{-(f-f_o)}{\tau} \qquad (6)$$

Each of these equations must be integrated over all k space or equivalently over energy using the density of states [15]. Before the integration is performed one more assumption must be made, that the relaxation time is independent of k or W. If the constant relaxation time assumption is not made then the energy dependence of the relaxation time must be moved through the gradient operator on the second term in each of equations (4-6) and a term accounting for the gradient of the relaxation time must be re-created. Changing the integration from k space to energy space, substituting for the mobility, ($\mu=\tau/m$), and making $v_g f_o$ equal to zero gives the following integral equations

$$\tau\frac{\partial(nv)}{\partial t} + \frac{2\mu}{3}\nabla g\int fW^{\frac{3}{2}}dW - \mu\frac{\nabla m_e}{m_e}g\int fW^{\frac{3}{2}}dW + \mu\nabla\epsilon_c g\int fW^{\frac{1}{2}}dW = -nv \qquad (7)$$

$$\tau\frac{\partial(nv)}{\partial t} + \frac{2\mu}{3}\nabla\left[g\int f\frac{(W\Upsilon)^{\frac{3}{2}}}{\Psi}dW\right] - \mu\frac{\nabla m_e}{m_e}g\int f\frac{(W\Upsilon)^{\frac{3}{2}}\left(1+\frac{4}{3}\alpha W\Upsilon\right)}{\Psi^3}dW$$
$$+ \mu\nabla\alpha g\int f\frac{W^2\left(-1+\frac{4}{3}\Upsilon^2\right)(W\Upsilon)^{\frac{1}{2}}}{\Psi^3}dW + \mu\nabla\epsilon_c g\int f\frac{(W\Upsilon)^{\frac{1}{2}}}{\Psi^2}dW = -nv \qquad (8)$$

$$\tau\frac{\partial(nv)}{\partial t} + \frac{2\mu\sqrt{x}}{3y}\nabla g\int fW^{\frac{y}{2}+1}dW + \frac{\mu\sqrt{x}\nabla m_e}{3y^2 m_e}[y-4]g\int fW^{\frac{y}{2}+1}dW + \frac{\mu\sqrt{x}\nabla x}{3xy^2}[y-4]g\int fW^{\frac{y}{2}+1}dW$$
$$+ \frac{\mu\sqrt{x}\nabla y}{y^3}g\int fW^{\frac{y}{2}+1}[-2-4\ln(W)+3y\ln(W)]dW + \mu\sqrt{x}\nabla\epsilon_c\left(\frac{2}{y}-1\right)g\int fW^{\frac{y}{2}}dW = -nv \qquad (9)$$

To produce closed form solutions for the integrals in equation (8) the binomial expansion is used repeatedly and all terms of order α^2 or higher are set to zero, to finally become

$$\tau\frac{\partial(nv)}{\partial t} + \frac{2\mu}{3}\nabla\left[g\int f\,W^{\frac{3}{2}}\left(1-\frac{\alpha W}{2}\right)dW\right] - \mu\frac{\nabla m_e}{m_e}g\int f\,W^{\frac{3}{2}}\left(1-\frac{19\alpha W}{6}\right)dW$$
$$+ \mu\nabla\alpha g\int f\,W^{\frac{5}{2}}\left(\frac{1}{3}+\frac{5\alpha W}{6}\right)dW + \mu\nabla\epsilon_c g\int f\,W^{\frac{1}{2}}\left(1-\frac{7\alpha W}{2}\right)dW = -nv \tag{10}$$

The only term in the power law flux equation (equation (9)) which will require an expansion is the ∇y term due to the ln(W) factor in the integrand. The expansion may only be required for certain choices of the distribution, but to maintain generality it is applied for all distributions. A parabolic interpolation, using the points 0, 0.5, and 1, to the part of the equation containing the log term is

$$\int fW^{\frac{y}{2}+1}\ln(W)\,dW \approx 4(0.5)^{\frac{y}{2}+1}\ln(0.5)\int f(W^2-W)\,dW \tag{11}$$

With the above substitution the power law flux equation can be written as

$$\tau\frac{\partial(nv)}{\partial t} + \frac{2\mu\sqrt{x}}{3y}\nabla g\int fW^{\frac{y}{2}+1}dW + \frac{\mu\sqrt{x}\nabla m_e}{3y^2 m_e}[y-4]g\int fW^{\frac{y}{2}+1}dW + \frac{\mu\sqrt{x}\nabla x}{3xy^2}[y-4]g\int fW^{\frac{y}{2}+1}dW$$
$$- \frac{2\mu\sqrt{x}\nabla y}{y^3}g\int fW^{\frac{y}{2}+1}dW + \frac{\mu\sqrt{x}\nabla y}{y^3}g[-4+3y]4\ln(0.5)(0.5)^{\frac{y}{2}+1}\int f(W^2-W)\,dW \tag{12}$$
$$+ \mu\sqrt{x}\nabla\epsilon_c\left(\frac{2}{y}-1\right)g\int fW^{\frac{y}{2}}dW = -nv$$

The approximation int equation (11) tends to degrade as y increases. However, this forcing term will not appear in simulations of homogeneous materials. In the case of inhomogeneous materials systems this term may be quite small as y has only a limited range, ($1 \leq y \leq 2$).

One of the goals of this paper is to derive a hydrodynamic model suitable for fast efficient simulation of state of the art devices. As previously stated the parabolic model is inadequate for certain material systems due to the fact that their band structures deviate dramatically from a parabolic shape at high energies. In these situations, a non-parabolic band structure provides a more accurate description. As discussed above, the full α formulation captures the desired physics, but is unattractive because the coefficients within the transport equations need to be numerically evaluated. In contrast, the binomial α formulation and the power law formulation provide closed form expressions for the transport coefficients. However, the question remains as to their ability to display the proper trends; how closely do the coefficients match the full α formulation? We will show that the binomial α formulation has a limited energy and non-parabolicity range due to the binomial approximation. Non-physical results will be obtained if the formulation is extended into regions outside the binomial limit. The power law does not produce non-physical results but more closely matches the parabolic formulation when fit to the low energy part of the band.

The coefficients on similar forcing terms in the various formulations can now be compared to examine the impact of the non-parabolicity factor and approximations made during the derivation. The comparison is done at this time to avoid any confusion from assuming a distribution function. Table I lists the forcing terms which are compared and the terms within the integrands involved. Table II contains the values of the non-parabolicity factors at which these factors are compared, this includes values of α from 0.04 to 4.0 and appropriate (x,y) values fit to these α values over two different energy ranges (0.0, 0.2) and (1.5, 3.0). Figure 3 shows the prefactor for the diffusion term from all the flux equations; Figure 3a is for slightly non-parabolic bands ($\alpha = 0.04$); 3b is for the non-parabolicity in reference [10] ($\alpha = 0.4789$), and 3c is for a highly non-parabolic band ($\alpha = 4.0$). Figures 4 a-c and 5 a-c display the prefactors on the forcing terms from changes in the effective mass and the field for the three degrees of non-parabolicity. For all three forcing terms at the lowest values of non-parabolicity (Figures 3a, 4a, 5a) the prefactors compare favorably with the parabolic formulation. For the diffusion term (Figures 3a-c) as the non-parabolicity factor increases the two cases of the power law formulation match very closely to the full α formulation. On the other hand the α formulation that utilizes the binomial expansion is very different, especially at the highest value of non-parabolicity considered. From Figure 3c it is clear that the binomial α formulation is clearly incorrect if the energy exceeds 0.5 eV. Even before this point the diffusion will be underestimated. In the case of the mass term, Figure 4, the power law formulation which is fit over the low energy range is much closer to the parabolic case, as expected due to the small change in the fitting parameters from their parabolic values. However, the power law with the parameters fit over a larger energy range more closely matches the full α formulation. As in the case of the diffusion term, the binomial α formulation severely underestimates the effect of this forcing term especially as the non-parabolicity is increased, and is limited to energies less than 0.1 eV for $\alpha = 4.0$. The coefficients for the field term, Figure 5, follow the same conclusions as for the mass term. From these figures it is clear that the binomial α formulation has a very limited energy range of validity as the non-parabolicity factor is increased. Using this formulation at higher energies or high non-parabolicity factors can give un-physical results due to the prefactors changing sign. On the other hand, the power law formulation with parameters fit over a small energy range will tend to produce results which more closely match the parabolic band model. It will not produce un-physical trends and does appear to have a larger range of validity for both energy and non-parabolicity factors. The case of the power law with parameters fit over a large energy range more closely matches the full α formulation in terms of the forcing coefficients. However, due to the problems previously described for the calculation of the carrier concentration this advantage may be immaterial.

Table I can also be used to gain some physical insights into transport in the non-parabolic band structures, especially using the power law formulation. First notice that as the non-parabolicity factor is decreased ($\alpha \rightarrow 0$, $x \rightarrow 1$, $y \rightarrow 1$) all the coefficients reduce to the parabolic case indicating that all three formulations are equivalent in this respect. As the non-parabolicity factor and energy increases the binomial α formulation can actually predict a change in the sign of a forcing term. In the full α formulation the sign on the forcing terms does not change but it is unclear as to how the term decreases. In the case of the power law, when the parameter y equals 2 it is obvious that the field term will become identically zero. The only terms which will be non-zero in the flux equation will be the diffusion, gradient in mass, and gradient in the non-parabolicity terms. This can be explained with the use of the power law energy equation {equation (1b)} and the group velocity equation. When y equals 2 there is a linear relationship between the momentum and energy, the bands are V shaped. The group velocity is proportional to the gradient of the energy with respect to k, which for the case of y equals 2 means that the group velocity is a constant. Therefore, no matter how much force is applied to the electron by external forces the velocity is not increased. The only factors which can produce current are gradients which can change this fixed velocity; i.e. changes in mass or non-parabolicity factor, or changes in the number of carriers moving at this fixed velocity, diffusion. Therefore, non-parabolic formulations which do not include coefficients to diminish the field term as the non-parabolicity increases overestimate the flux.

At this point in the derivation a recursion relation must be formulated, a distribution function assumed, or some other mathematical method {Minimum-Maximum theorem} must be used to provide mathematical closure for equations (7), (10), and (12). Since, a goal of this paper is the formulation of models suitable for the numerical simulation of devices the first two options are explored [16]. A recursion relation would allow moments of higher order to be approximated by lower order moments, the lower orders are calculated from the conservation equations. This option does not require that a specific form of the distribution function be used, unless the recursion relations are based on a specific distribution. However, in the case of non-parabolic bands the standard recursion relations may no longer be applicable [9]. Therefore, this option was not pursued. The other option, and the one chosen for this work, is to assume a specific form for the distribution function, higher moments can then be calculated based on the known distribution function. Some of the choices for the distribution function include heated Maxwellian, shifted and heated Maxwellian, heated Fermi-Dirac, or shifted and heated Fermi-Dirac. Since the Maxwellian distributions can be recovered by relaxing the degeneracy, the Fermi-Dirac distributions were the only ones considered for this work.

In the non-parabolic formulation a simple relation between energy and velocity will not exist due to the change in the density of states. Also higher order powers of the energy are required to close the relationships in the α formulation, this will require cross product terms involving the temperature and the velocity. In addition, the power law formulation has non-integer powers of the energy which will be very difficult to evaluate for the shifted and heated distributions. Due to these conditions and the fact that all the formulations break down as the energy rises, the heated Fermi-Dirac distribution was used to close the relationships. The flux equation in the binomial α formulation is

$$
\begin{aligned}
-n\bar{v} = {} & \mu K T_e \left[\frac{\mathcal{F}^2_{\frac{1}{2}} + \frac{10}{4}\alpha K T_e \mathcal{F}_{\frac{3}{2}} \mathcal{F}_{\frac{1}{2}}}{\mathcal{F}_{\frac{1}{2}} \mathcal{F}_{-\frac{1}{2}} + \frac{15}{4}\alpha K T_e \left(\mathcal{F}^2_{\frac{1}{2}} + \frac{\mathcal{F}_{-\frac{1}{2}} \mathcal{F}_{\frac{3}{2}}}{2} \right)} \right] \nabla n + \mu n \left[\frac{\mathcal{F}_{\frac{1}{2}} - \frac{21}{4}\alpha K T_e \mathcal{F}_{\frac{3}{2}}}{\Omega} \right] \nabla \epsilon_c \\
& - \frac{\mu n K T_e}{\Lambda} \left[\mathcal{F}_{\frac{1}{2}} + \frac{\mathcal{F}^2_{\frac{1}{2}} + 20\alpha K T_e \mathcal{F}_{\frac{5}{2}} \mathcal{F}_{-\frac{1}{2}}}{2\Omega} \right] \frac{\nabla m}{m} + \frac{\mu n K T_e}{\Lambda \Omega} \left[\frac{5}{2} \mathcal{F}_{-\frac{1}{2}} \mathcal{F}_{\frac{3}{2}} - \mathcal{F}^2_{\frac{1}{2}} - \frac{\mathcal{F}^3_{\frac{1}{2}}}{2\Omega} \right] \frac{\nabla T_e}{T_e} \\
& - \frac{4\mu n (K T_e)^2}{\Omega} \left[\frac{10 \mathcal{F}_{\frac{1}{2}} \mathcal{F}_{\frac{3}{2}}}{\Lambda} - \frac{175}{4}\alpha K T_e \mathcal{F}_{\frac{7}{2}} + \frac{\mathcal{F}^2_{\frac{1}{2}} \mathcal{F}_{\frac{3}{2}}}{\Lambda \Omega} \right] \nabla \alpha
\end{aligned}
\qquad (13)
$$

The flux equation in the power law formulation becomes

$$
\begin{aligned}
-n\bar{v} ={}& \frac{2\mu}{3xy^2}(KT_e)^{2-y}\frac{\left(\frac{y}{2}+1\right)\Gamma\left(\frac{y}{2}+1\right)\mathcal{F}_{\frac{y}{2}}}{\left(\frac{3}{2}y-1\right)\Gamma\left(\frac{3}{2}y-1\right)\mathcal{F}_{\frac{3}{2}y-2}}\nabla n+\frac{(2-y)\mu n}{xy^2}(KT_e)^{1-y}\frac{\Gamma\left(\frac{y}{2}+1\right)\mathcal{F}_{\frac{y}{2}}}{\Gamma\left(\frac{3}{2}y\right)\mathcal{F}_{\frac{3}{2}y-1}}\nabla\epsilon_c \\
&+\frac{\mu n}{xy^2}(KT_e)^{2-y}\left[\frac{-y\left(\frac{y}{2}+1\right)\Gamma\left(\frac{y}{2}+1\right)\mathcal{F}_{\frac{y}{2}}}{\left(\frac{3}{2}y-1\right)\Gamma\left(\frac{3}{2}y-1\right)\mathcal{F}_{\frac{3}{2}y-2}}+\frac{(4+y)\Gamma\left(\frac{y}{2}+2\right)\mathcal{F}_{\frac{y}{2}+1}}{3\Gamma\left(\frac{3}{2}y\right)\mathcal{F}_{\frac{3}{2}y-1}}\right]\frac{\nabla T_e}{T_e} \\
&-\frac{\mu n}{xy^2}(KT_e)^{2-y}\left[\frac{\left(\frac{y}{2}+1\right)\Gamma\left(\frac{y}{2}+1\right)\mathcal{F}_{\frac{y}{2}}}{\left(\frac{3}{2}y-1\right)\Gamma\left(\frac{3}{2}y-1\right)\mathcal{F}_{\frac{3}{2}y-2}}-\frac{4\Gamma\left(\frac{y}{2}+2\right)\mathcal{F}_{\frac{y}{2}+1}}{3\Gamma\left(\frac{3}{2}y\right)\mathcal{F}_{\frac{3}{2}y-1}}\left(1-\frac{1}{y}\right)\right]\left(\frac{\nabla m}{m}+\frac{\nabla x}{x}\right) \\
&+\frac{\mu n}{xy^3}(KT_e)^{2-y}\left[\frac{-2\left(\frac{y}{2}+1\right)\Gamma\left(\frac{y}{2}+1\right)\mathcal{F}_{\frac{y}{2}}}{3\left(\frac{3}{2}y-1\right)\Gamma\left(\frac{3}{2}y-1\right)\mathcal{F}_{\frac{3}{2}y-2}}\left(1+\frac{3}{2}y\ln(KT_e)\right)+\frac{\Gamma\left(\frac{y}{2}+2\right)\mathcal{F}_{\frac{y}{2}+1}}{3\Gamma\left(\frac{3}{2}y\right)\mathcal{F}_{\frac{3}{2}y-1}}(-4+y\ln(KT_e))\right. \\
&\left.+(3y-4)4\ln(0.5)(0.5)^{\frac{y}{2}+1}(KT_e)^{-\frac{y}{2}}\left(\frac{KT_e\Gamma(3)\mathcal{F}_2-\Gamma(2)\mathcal{F}_1}{\Gamma\left(\frac{3}{2}y\right)\mathcal{F}_{\frac{3}{2}y-1}}\right)\right]\nabla y
\end{aligned}
\tag{14}
$$

The reader can verify that as the non-parabolicity factors are diminished, (α→0, x,y→1), the two non-parabolic formulations reduce to the standard parabolic case. The equations also reduce to simpler forms when the degeneracy effects are ignored (all orders of Fermi integral reduce to exponentials). The flux equations can be discretized using normal techniques to produce comparable simulation codes under various assumptions [17].

Energy Flux Equations

For the energy flux equation ($\Theta = Wv_g$) the general conservation equation is

$$
\begin{aligned}
&\frac{\partial}{\partial t}\left(W\overline{\upsilon_g}f\right)+\nabla\cdot\left(fW\overline{\upsilon_g\upsilon_g}\right)-f\overline{\upsilon_g\upsilon_g}\cdot\nabla W-fW\frac{\hbar^2(kk)}{m(k)}\cdot\nabla\left(\frac{1}{m(W)}\right) \\
&-fF\cdot\overline{\upsilon_g\upsilon_g}-f\overline{F}\cdot\frac{W}{m(k)}I+fF\cdot\frac{3W(k\nabla_k m(k))}{m(k)^2}=W\overline{\upsilon_g}\frac{-(f-f_0)}{\tau}
\end{aligned}
\tag{15}
$$

Notice that the fourth through seventh terms on the left hand side are tensor products. As in the case of the particle flux moment the energy flux moment equation can not be processed further until some functional form of the effective mass is assumed. By making similar assumptions, substitutions, and approximations {binomial expansion, Fermi-Dirac statistics, equipartition of energy ...} the energy flux equations for the three dispersion relationships become

$$-\bar{S} = \frac{5}{2}\mu n K T_e \left[K T_e \left[\frac{\mathcal{F}_{\frac{3}{2}}}{\mathcal{F}_{-\frac{1}{2}}} \right] \frac{\nabla n}{n} + \left[\frac{\mathcal{F}_{\frac{3}{2}}}{\mathcal{F}_{\frac{1}{2}}} \right] \nabla \epsilon_c - \frac{3 K T_e}{2} \left[\frac{\mathcal{F}_{\frac{3}{2}}}{\mathcal{F}_{-\frac{1}{2}}} \right] \frac{\nabla m}{m} + \frac{7}{2} K T_e \frac{\mathcal{F}_{\frac{5}{2}}}{\mathcal{F}_{\frac{1}{2}}} \left[1 - \frac{3}{7} \frac{\mathcal{F}_{\frac{1}{2}} \mathcal{F}_{\frac{3}{2}}}{\mathcal{F}_{-\frac{1}{2}} \mathcal{F}_{\frac{5}{2}}} \right] \frac{\nabla T_e}{T_e} \right] \tag{16}$$

$$\begin{aligned} -\bar{S} = {} & \frac{5\mu (K T_e)^2}{2} \left[\frac{\mathcal{F}_{\frac{3}{2}} \Omega - \frac{7}{4} \alpha K T_e \mathcal{F}_{\frac{1}{2}} \mathcal{F}_{\frac{5}{2}}}{\Lambda \Omega} \right] \nabla n + \frac{5 \mu n K T_e}{2} \left[\frac{\mathcal{F}_{\frac{3}{2}} - \frac{23}{4} \alpha K T_e \mathcal{F}_{\frac{5}{2}}}{\Omega} \right] \nabla \epsilon_c \\ & - \frac{5 \mu n (K T_e)^2}{2} \left[\frac{3 \mathcal{F}_{\frac{3}{2}}}{2\Lambda} - \frac{14 \alpha K T_e \mathcal{F}_{\frac{7}{2}}}{\Omega} - \frac{21 \alpha K T_e \mathcal{F}_{\frac{5}{2}} \mathcal{F}_{\frac{1}{2}}}{8 \Lambda \Omega} \right] \frac{\nabla m}{m} \\ & + \frac{5 \mu n (K T_e)^2}{2 \Omega} \left[\frac{5}{2} \mathcal{F}_{\frac{5}{2}} - \frac{21}{8} \alpha K T_e \mathcal{F}_{\frac{7}{2}} + \frac{\mathcal{F}_{\frac{1}{2}} \mathcal{F}_{\frac{5}{2}} - \frac{3}{20} \alpha K T_e \mathcal{F}_{\frac{1}{2}} \mathcal{F}_{\frac{3}{2}}}{\Omega} - \frac{3 \mathcal{F}_{\frac{3}{2}} \Omega - \frac{101}{8} \alpha K T_e \mathcal{F}_{\frac{1}{2}} \mathcal{F}_{\frac{5}{2}}}{2\Lambda} \right] \frac{\nabla T_e}{T_e} \\ & - \frac{5 \mu n (K T_e)^3}{2 \Omega} \left[\frac{3 \mathcal{F}_{\frac{3}{2}}^2}{2\Lambda} - \frac{315}{16} \alpha K T_e \mathcal{F}_{\frac{9}{2}} + \frac{105 \alpha K T_e \mathcal{F}_{\frac{1}{2}} \mathcal{F}_{\frac{3}{2}} \mathcal{F}_{\frac{5}{2}}}{16 \Lambda \Omega} \right] \nabla \alpha \end{aligned} \tag{17}$$

$$\begin{aligned}-\bar{S} = {}& \frac{2\mu}{3xy^2}(KT_e)^{3-y}\frac{\left(\frac{y}{2}+2\right)\Gamma\left(\frac{y}{2}+2\right)\mathcal{F}_{\frac{y}{2}+1}}{\left(\frac{3}{2}y-1\right)\Gamma\left(\frac{3}{2}y-1\right)\mathcal{F}_{\frac{3}{2}y-2}}\nabla n + \frac{(8-3y)\mu n}{3xy^2}(KT_e)^{2-y}\frac{\Gamma\left(\frac{y}{2}+2\right)\mathcal{F}_{\frac{y}{2}+1}}{\Gamma\left(\frac{3}{2}y\right)\mathcal{F}_{\frac{3}{2}y-1}}\nabla\epsilon_c \\ & + \frac{\mu n}{xy^2}(KT_e)^{3-y}\left[\frac{-y\left(\frac{y}{2}+2\right)\Gamma\left(\frac{y}{2}+2\right)\mathcal{F}_{\frac{y}{2}+1}}{\left(\frac{3}{2}y-1\right)\Gamma\left(\frac{3}{2}y-1\right)\mathcal{F}_{\frac{3}{2}y-2}} + \frac{(6+y)\Gamma\left(\frac{y}{2}+3\right)\mathcal{F}_{\frac{y}{2}+2}}{3\Gamma\left(\frac{3}{2}y\right)\mathcal{F}_{\frac{3}{2}y-1}}\right]\frac{\nabla T_e}{T_e} \\ & - \frac{\mu n}{xy^2}(KT_e)^{3-y}\left[\frac{\left(\frac{y}{2}+2\right)\Gamma\left(\frac{y}{2}+2\right)\mathcal{F}_{\frac{y}{2}+1}}{\left(\frac{3}{2}y-1\right)\Gamma\left(\frac{3}{2}y-1\right)\mathcal{F}_{\frac{3}{2}y-2}} - \frac{4\Gamma\left(\frac{y}{2}+3\right)\mathcal{F}_{\frac{y}{2}+2}}{3\Gamma\left(\frac{3}{2}y\right)\mathcal{F}_{\frac{3}{2}y-1}}\left(1-\frac{1}{y}\right)\right]\left(\frac{\nabla m}{m}+\frac{\nabla x}{x}\right) \qquad (18) \\ & + \frac{\mu n}{xy^3}(KT_e)^{3-y}\left[\frac{-2\left(\frac{y}{2}+2\right)\Gamma\left(\frac{y}{2}+2\right)\mathcal{F}_{\frac{y}{2}+1}}{3\left(\frac{3}{2}y-1\right)\Gamma\left(\frac{3}{2}y-1\right)\mathcal{F}_{\frac{3}{2}y-2}}\left(1+\frac{3}{2}y\ln(KT_e)\right) + \frac{\Gamma\left(\frac{y}{2}+3\right)\mathcal{F}_{\frac{y}{2}+2}}{3\Gamma\left(\frac{3}{2}y\right)\mathcal{F}_{\frac{3}{2}y-1}}(-4+y\ln(KT_e))\right. \\ & \left. + (3y-4)4\ln(0.5)(0.5)^{\frac{y}{2}+2}(KT_e)^{-\frac{y}{2}+1}\left(\frac{KT_e\Gamma(3)\mathcal{F}_2-\Gamma(2)\mathcal{F}_1}{\Gamma\left(\frac{3}{2}y\right)\mathcal{F}_{\frac{3}{2}y-1}}\right)\right]\nabla y\end{aligned}$$

First, equation (16) corrects a sign error on the order of a Fermi integral which occurred in an earlier publication [17]. Again, the reader can verify that the non-parabolic formulations reduce to the parabolic case as the non-parabolicity factors are decreased. As in the case of the particle flux equations the energy flux equations can be discretized using normal techniques [17].

CONCLUSIONS

Two formulations of the hydrodynamic model have been presented for the simulation of non-parabolic inhomogeneous material systems, the standard Kane formulation and the power law formulation of Cassi and Riccò. Both forms reduce to the parabolic hydrodynamic model as the non-parabolicity factors are diminished. The forcing terms in the particle and energy flux equations due to variations in the non-parabolicity factors of the bands as suggested by Azoff have been re-created in both non-parabolic formulations. It was shown that the binomial α formulation is suitable for the calculation of the carrier concentration but has a limited energy and non-parabolicity range when applied to the coefficients of the flux equations. Extending the binomial α formulation past these limits leads to non-physical terms in both the particle and energy flux equations. In the case of the power law formulation it was shown that when the adjustable parameters were fit to the high energy range the deviation in the carrier concentration from both the parabolic and α cases was extreme. When fit to the lower energy range the power law produced carrier concentrations comparable to the α formulations. The energy and non-parabolicity range of the power law formulation for the particle and energy flux equations is larger than the binomial α formulation, but it is still limited by the adjustable parameters. However, unlike the binomial α formulation the power law will not lead to physically unrealistic results, but will tend to more closely match the parabolic formulation when the adjustable parameters are fit over the low energy portion of the band. It is shown and argued using the power law formulation and a high non-parabolicity factor ($y = 2$) that a dampening factor must exist on the field term in the particle flux equation to account for the non-parabolicity of the bands in both non-parabolic formulations. Particle flux and energy flux equations using a heated Fermi-Dirac distribution function are also presented, to allow for incorporation into existing device simulators.

ACKNOWLEDGEMENTS

This work was sponsored in part by ARPA through contract to NASA, NAGW-2753, the National Science Foundation through grant ECS-9313635, and by ARPA through the Phosphor Technology Center of Excellence, Contract MDA972-93-1-0030.

REFERENCES

1. G. Dresselhaus, Phys. Rev., Vol. 100, pp. 580, (1955).
2. R. H. Parmenter, Phys. Rev., Vol. 100, pp. 573, (1955).
3. E. O. Kane, J. Phys. Chem. Solids, Vol. 1, pp. 249, (1957).
4. R. A. Stewart and J. N. Churchill, Solid State Electronics, Vol 33, #7, pp. 819, (1990).
5. R. Thoma, A. Emunds, B. Meinerzhagen, H.-J. Peifer, and W. L. Engl, IEEE Trans Elec. Dev., Vol. 38, #6, pp. 1343, (1991).
6. T. J. Bordelon, X.-L. Wang, C. M. Maziar, and A. F. Tasch, Solid State Elec., Vol. 35, #2, pp. 131, (1992).
7. D. Chen, E. C. Kan, U. Ravaioli, C.-W. Shu, and R. W. Dutton, IEEE Elec. Dev. Letts., Vol. 13, #1, pp. 26, (1992).
8. E. M. Azoff, J. Appl. Phys., Vol. 64, #5, pp. 2439, (1988).
9. D. L. Woolard, H. Tain, R. J. Trew, M. A. Littlejohn, and K. W. Kim, Phys. Rev. B, Vol. 44, #20, pp. 11119, (1991).
10. D. Cassi and B. Riccò, IEEE Trans Elec. Dev., Vol. 37, #6, pp. 1514, (1990).
11. H. B. Bebb and C. R. Ratliff, J. Appl. Phys., Vol. 42, #8, pp. 3189, (1971).
12. E. M. Azoff, COMPEL, Vol. 6, #1, pp. 25, (1987).
13. C. C. McAndrew, E. L. Heasell, and K. Singhal, Semicond. Sci. Technol., Vol. 2, pp. 643, (1987).
14. R. Kishore, Physica A, Vol. 196, pp. 133, (1993).
15. N. W. Ashcroft and N. D. Merman, Solid State Physics, Holt, Rinehart and Winston, N. Y., N. Y., (1976).
16. J. Higman and K. Hess, Solid State Elec., Vol. 29, #9, pp. 915, (1986).
17. A. W. Smith and A. Rohatgi, IEEE Trans. Computer Aided Design and Integated Circuits, Vol. 12, #10, pp. 1515, (1993).

Table I. Terms (prefactors) within the integrands of the forcing coefficients which are graphically compared.

Formulation	Equation Number	Diffusion Term	Mass Term ∇m	Field Term $\nabla \varepsilon_o$
parabolic	(7)	$W^{\frac{3}{2}}$	$W^{\frac{3}{2}}$	$W^{\frac{1}{2}}$
α formulation	(8)	$\frac{(W(1+\alpha W))^{\frac{3}{2}}}{(1+2\alpha W)}$	$\frac{(W(1+\alpha W))^{\frac{3}{2}}(1+4\alpha W)}{(1+2\alpha W)^3}$	$\frac{W^{\frac{1}{2}}(1+\alpha W)^{\frac{1}{2}}}{(1+2\alpha W)^2}$
α with binomial expansion used	(10)	$W^{\frac{3}{2}}\left(1-\frac{\alpha W}{2}\right)$	$W^{\frac{3}{2}}\left(1-\frac{19\alpha W}{6}\right)$	$W^{\frac{1}{2}}\left(1-\frac{7\alpha W}{2}\right)$
power law	(12)	$\frac{x^{\frac{1}{2}}}{y}W^{1+\frac{y}{2}}$	$\frac{x^{\frac{1}{2}}}{3y^2}[4-y]W^{1+\frac{y}{2}}$	$x^{\frac{1}{2}}\frac{(2-y)}{y}W^{\frac{y}{2}}$

Table II. Values of the non-parabolicity factors which are compared. This includes α values from 0.04 to 4.0 and (x,y) values fit to these α values over two different energy ranges (0.0, 0.2) and (1.5, 3.0).

Case	α	x, y {0.0, 0.2}	x, y {1.5, 3.0}
a	0.04	1.0148, 1.0045	1.0207, 1.0827
b	0.4789	1.185,1.052	1.365, 1.52
c	4.0	2.975,1.322	4.8233, 1.901

Figure Captions

Figure 1. Dispersion relations for the Kane model (solid line, $\alpha = 0.4789$), the power law formulation (dashed line, $x=1.365$, $y = 1.52$ fit over high energy, $1.5 \leq W \leq 3.0$ eV) and the power law formulation (dotted line, $x=1.185$, $y = 1.052$ fit over low energy, $0.0 \leq W \leq 0.2$ eV). The insert shows the detail of the low energy range.

Figure 2. Deviation, from the parabolic case, of the carrier concentration as a function of the reduced energy for the full α formulation (solid line, $\alpha = 0.4789$), binomial α (dotted), power law fit at high energy (dashed, $x=1.365$, $y=1.52$), and power law fit at low energy (dashed, $x=1.185$, $y=1.052$) dispersion relations as a function of the reduced energy (η) at $T_e=300$ K.

Figure 3. Comparison of the integrand coefficients (prefactors) occurring on the diffusion term of the particle flux formulations. See Table I and II for the exact form of the equations and degrees of non-parabolicity considered.

Figure 4. Comparison of the integrand coefficients (prefactors) occurring on the gradient of the effective mass term of the particle flux formulations. See Table I and II for the exact form of the equations and degrees of non-parabolicity considered.

Figure 5. Comparison of the integrand coefficients (prefactors) occurring on the gradient of the potential term occurring in the particle flux formulations. See Table I and II for the exact form of the equations and degrees of non-parabolicity considered.

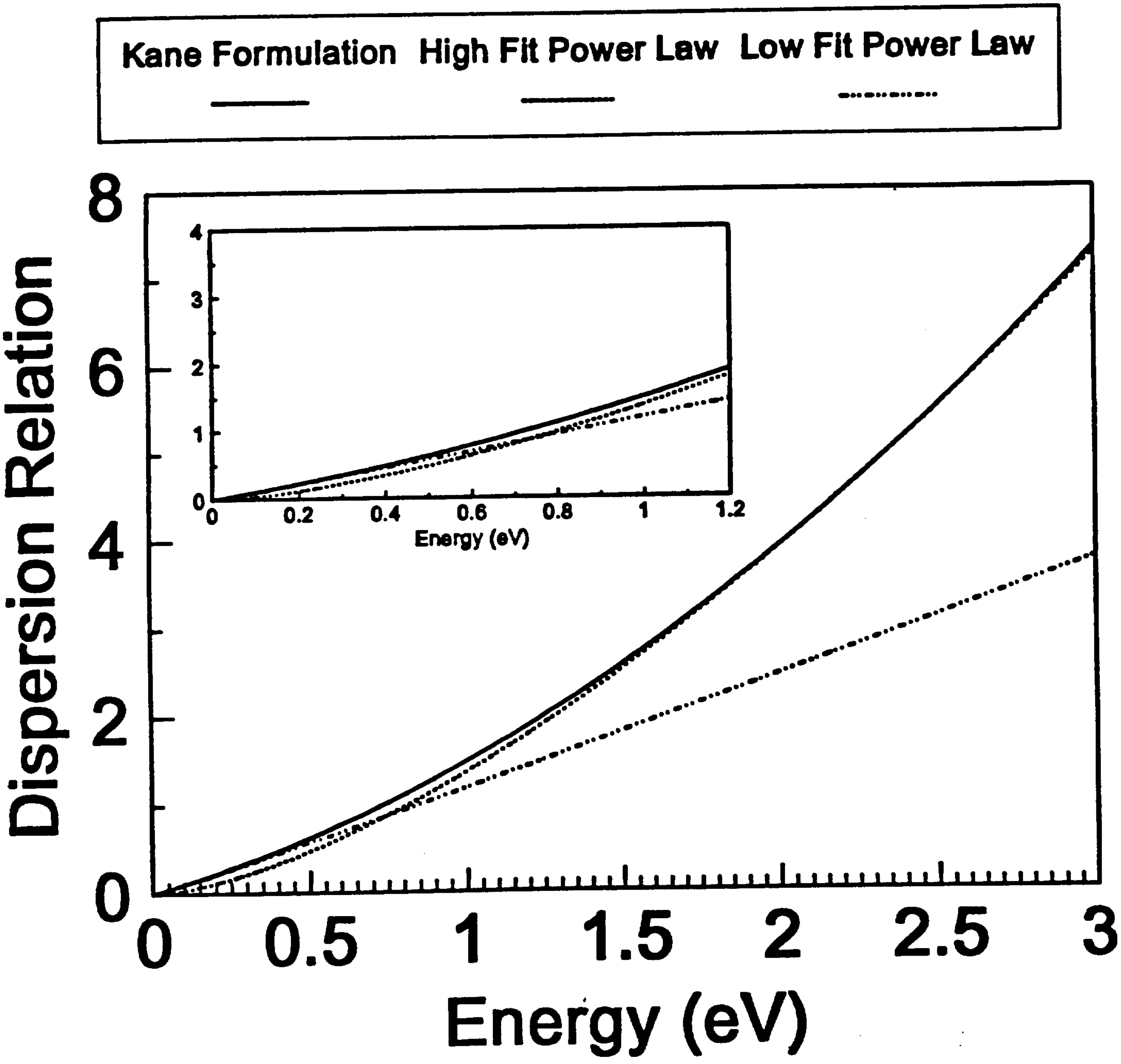

Smith, Brennan "Non-Parabolic...." Fig. 1

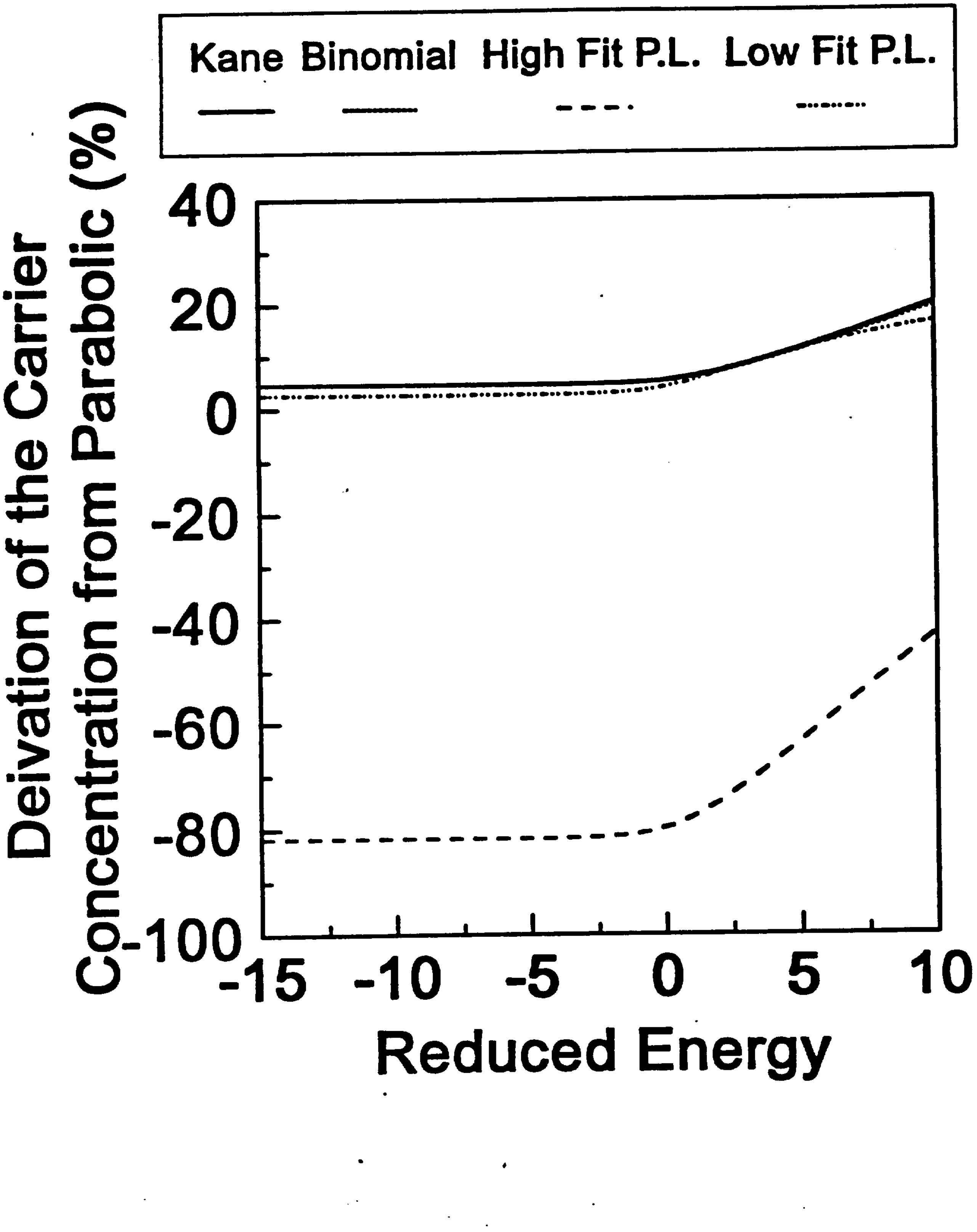

Smith, Brennan "Non-Parabolic...." Fig. 2

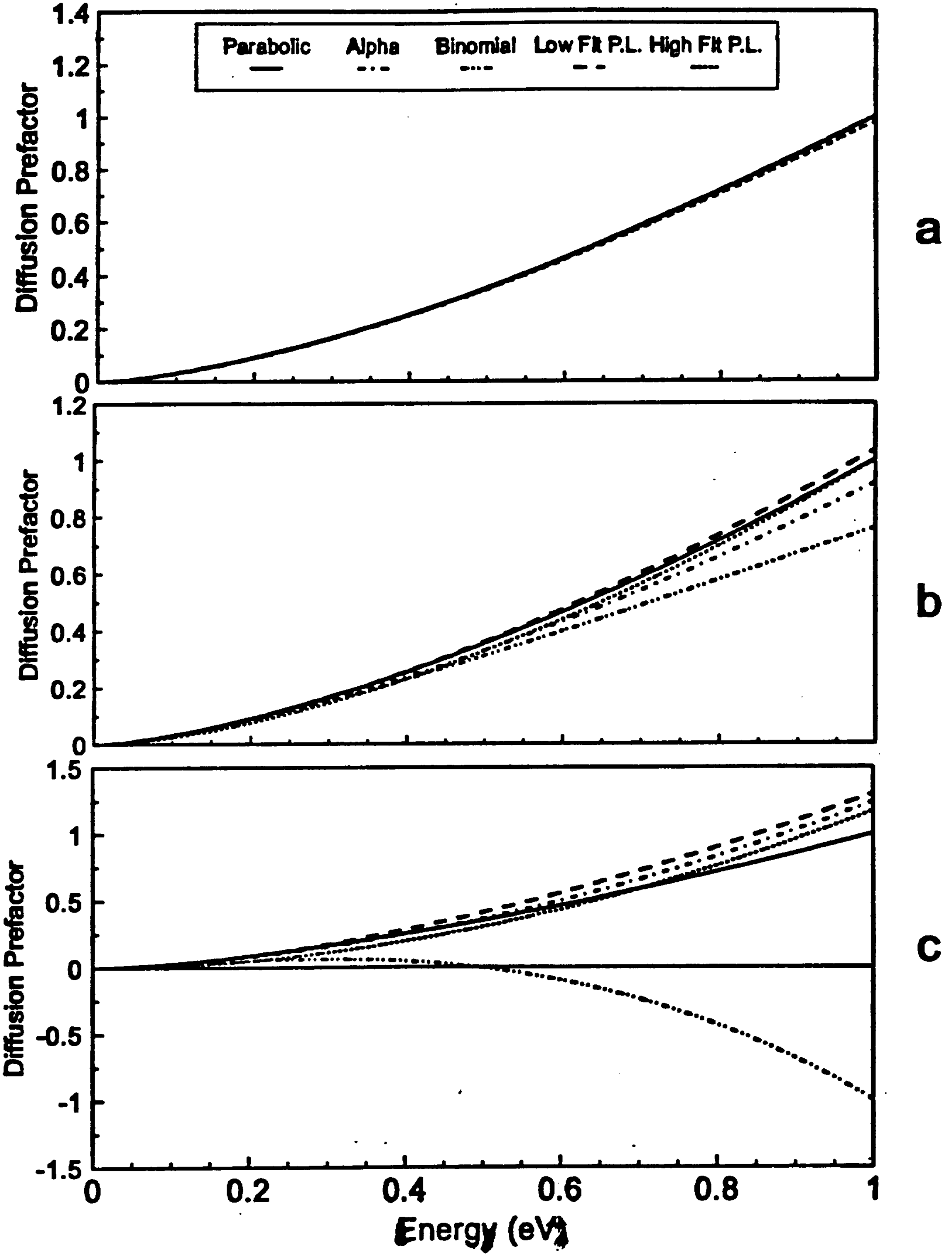

Smith, Brennan "Non-Parabolic...." Fig. 3

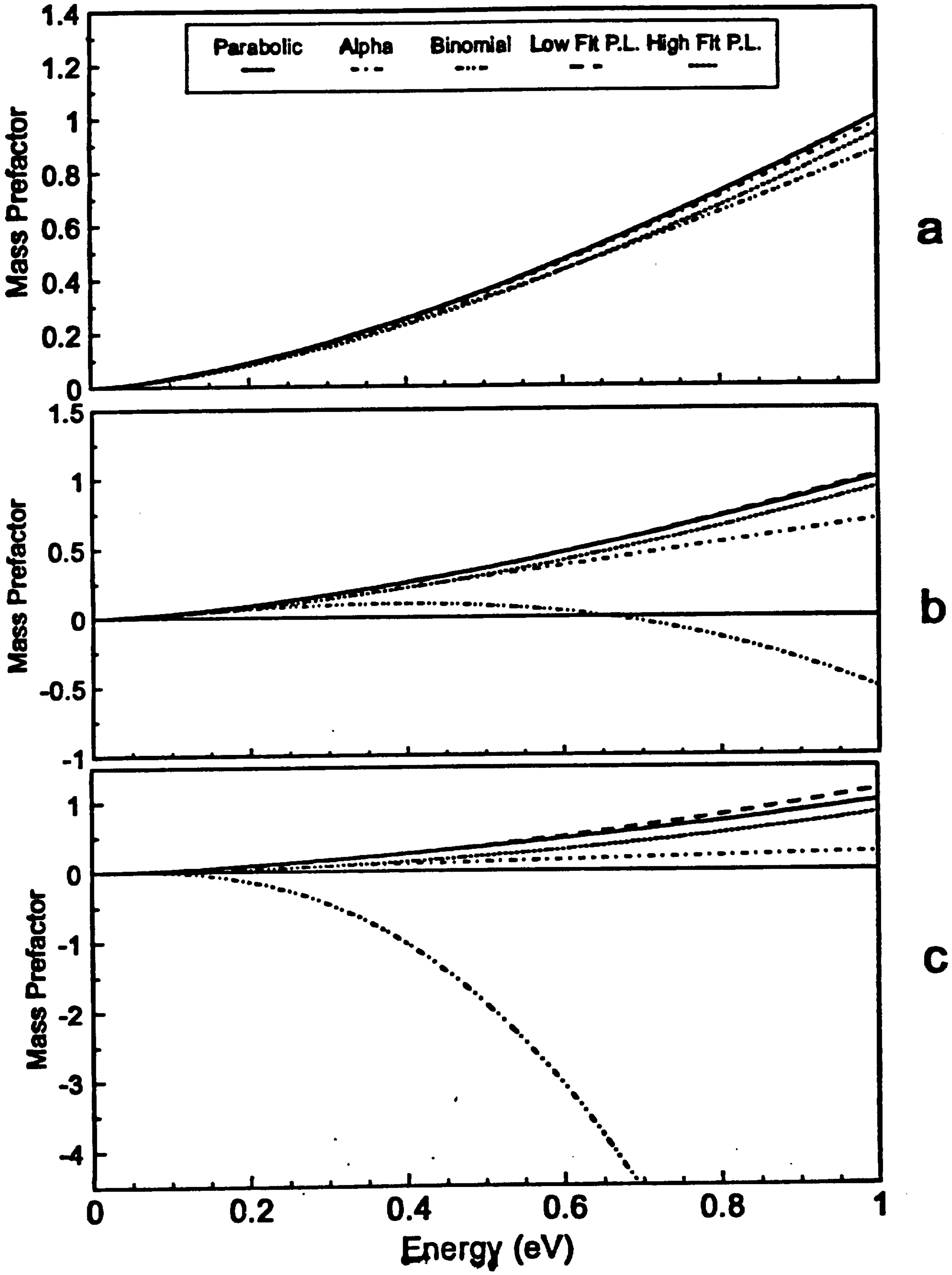

Smith, Brennan "Non-Parabolic...." Fig. 4

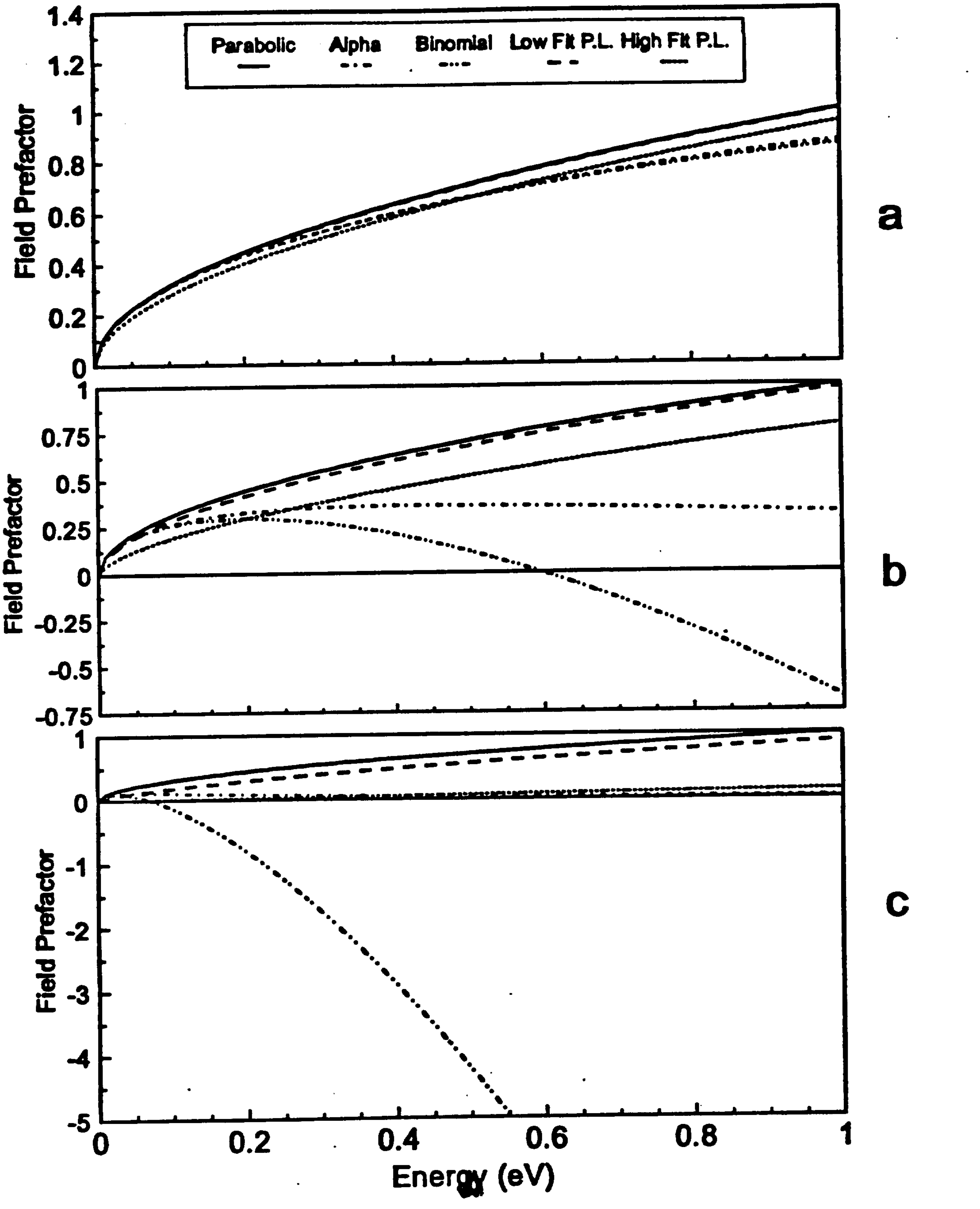

Smith, Brennan "Non-Parabolic...." Fig. 5